Vision based Navigation, Guidance and Control of 6 DOF Robotic manipulator for Space Berthing application

Mr. Jayanta Laha
Scientist/ Engineer, Indian Space Research Organization
jayantalaha@leos.gov.in

Mr. Abhinandan Kapoor
Scientist/ Engineer, Indian Space Research Organization
akapoor@ursc.gov.in

Mr. Amit Maji
Scientist/ Engineer, Indian Space Research Organization
amit@leos.gov.in

Mr Ayush Kejriwal
Scientist/ Engineer, Indian Space Research Organization
,ayush@ursc.gov.in

Mr Sidhharth Tiwari
Scientist/ Engineer, Indian Space Research Organization
sidharth@ursc.gov.in

Mr Subash Yadav
Scientist/ Engineer, Indian Space Research Organization
syadav@ursc.gov.in

Mr. Abhishek Kumar
Scientist/ Engineer, Indian Space Research Organization
abhishek@ursc.gov.in

Dr. B. P. Nagaraj
Scientist/ Engineer, Indian Space Research Organization
bpn@ursc.gov.in

H. N. Suresha Kumar
Scientist/ Engineer, Indian Space Research Organization
hns@ursc.gov.in

ABSTRACT

Berthing of the spacecraft with non cooperative targets are gaining interest in recent days. Space robotics is considered one of the most promising approaches for missions such as docking, refuelling, repairing, upgrading, transporting, rescuing, and orbital debris removal. Many enabling techniques have been developed in the past two decades and several technology demonstration missions have been completed. A number of manned on-orbit servicing missions were successfully accomplished but unmanned, fully autonomous, non-co-operative servicing missions have not been done yet. With the advent of advanced image processing algorithm and its hardware implementation made it possible to perform robotic arm actuations in space for berthing with on orbit satellite. Usually the robotic arm will be equipped by a small camera which will track the target. Here the usage of colour marker is useful as it can be detected and tracked faster with less amount of processing. One of the greatest challenges is to ensure the servicing spacecraft safely and reliably docks with the target spacecraft or capture the target to stabilize it for subsequent berthing. This is especially important if the target has an unknown motion and kinematics/ dynamics.

CCS CONCEPTS

• **Hardware** → Communication hardware, interfaces and storage; Sensor applications and deployments; • **Computing methodologies** → Artificial intelligence; Computer vision; Computer vision problems; Tracking.

KEYWORDS

Keywords—Berthing, Chaser, Target, Robotic Arm, colour tracking,6DOF, Revolute Joints, BLDC Motors, Gripper

ACM Reference Format:
Mr. Jayanta Laha, Mr. Abhinandan Kapoor, Mr. Amit Maji, Mr Ayush Kejriwal, Mr Sidhharth Tiwari, Mr Subash Yadav, Mr. Abhishek Kumar, Dr. B. P. Nagaraj, and H. N. Suresha Kumar. 2023. Vision based Navigation, Guidance and Control of 6 DOF Robotic manipulator for Space Berthing application. In *Advances In Robotics - 6th International Conference of The Robotics Society (AIR 2023), July 05–08, 2023, Ropar, India.* ACM, New York, NY, USA, 9 pages. https://doi.org/10.1145/3610419.3610492

Publication rights licensed to ACM. ACM acknowledges that this contribution was authored or co-authored by an employee, contractor or affiliate of a national government. As such, the Government retains a nonexclusive, royalty-free right to publish or reproduce this article, or to allow others to do so, for Government purposes only.

AIR 2023, July 05–08, 2023, Ropar, India

© 2023 Copyright held by the owner/author(s). Publication rights licensed to ACM.

ACM ISBN 978-1-4503-9980-7/23/07…$15.00
https://doi.org/10.1145/3610419.3610492

1 INTRODUCTION

Space Robotics deals with the development of general purpose machines that are capable of surviving the rigors of the space environment and perform exploration, assembly, construction, maintenance, servicing or other tasks. Space Robots are generally designed to do multiple tasks, like payload deployment, retrieval, inspections and planetary exploration including unanticipated operations [1].Space robotics has shown immense potential in the recent years due to comparatively lower cost and lower risk factors for manned missions. In addition, it has supported several on-orbit operations to astronauts on-board, thus emphasizing its importance. One such important application of space robotics is docking. Docking and undocking of spacecraft are required for replenishment of fuel, propellant, power, food or maintenance for space systems. Presently, two types of docking concepts are in practice. In the first type, the relative velocities between the chaser and target spacecraft are used to activate the docking mechanism (Figure 1) and it is known as "Impact Docking". Typically, rigid spacecraft which are axis-symmetric have employed this concept. The second type of docking is the low impact docking concept. This concept induces low docking disturbance at the time of contact and the risk of damage to the spacecraft due to collision is minimal [2, 3]. Berthing falls in the category of low impact docking concepts. The 'Berthing' scheme [4, 9] refers to the use of an intermediate system, typically a robotic arm to capture the target vehicle. Further, the robotic arm performs

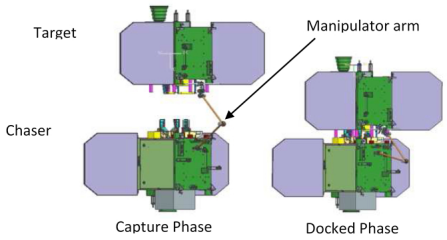

Figure 1: Target and Chaser spacecraft with manipulator

the maneuvers required to position the vehicles for the desired interface and subsequently docks the target Spacecraft to chaser Spacecraft by means of motor driven latches provided on the chaser spacecraft. The Space Shuttle manipulator/robotic arm is a classic example for berthing. In this approach, the risk due to collision is minimized. A dexterous robotic arm is useful for controlling a non-cooperative target with greater accuracy and alignment [5, 6]. ETS-7-Orbital [7] Rendezvous & Robotic Mission (JAXA), Orbital Express, Dexterous Robotic arm (ESA), JEM Remote manipulator system (JAXA), European Robotic arm (ERA), SSRMS (Canada Arm-2) are examples of Berthing scheme for low impact docking. In this paper, then overall processing pipeline is explained .Initially vision based method is used to detect the marker and 6DOF is found out.To motivate and facilitate such research and development, this paper provides a literature review related to the kinematics, dynamics, control and verification of space robotic systems, the requirement and best positions to mount the marker, image processing pipeline for vision based target marker acquisition to compute their co-ordinates, 6DOF(degree of freedom) computation, motor selection, design, analysis and test envisaged for the development robotic arm and robotic arm gripper design and its actuation is presented.

2 LITERATURE SURVEY

In recent times, due to advancement of vision based system availability with good processing power, berthing and on-orbit servicing (OOS) of the spacecraft has gain interest over the researchers. [11, 13, 14]These research works were motivated by several national and international missions not only for repairing, rescuing, and refuelling failed satellites, but also for removal of defunct satellites or space debris [12, 17]. A space robotic system (also referred to as space manipulator or space robot) for an OOS mission typically consists of three major components: the base spacecraft or servicing satellite, an n degree-of-freedom (n-DOF) robot manipulator attached to the servicing satellite, and the target spacecraft to be serviced. A spacecraft-manipulator servicing vehicle is sometimes termed the servicing system. The capturing process includes a series of operations. After having completed the far and close-range rendezvous manoeuvres [13] with the target satellite, the servicing spacecraft remains at a safe, station-keeping, distance from the tumbling target satellite. Then, the capture operation mode starts, which may be divided into four phases. The first phase corresponds to the observing and planning phase for acquiring motion and physical properties information about the target satellite, to plan how the robot manipulator should grasp the target. In this stage vision based algorithms are used to identify the target spacecraft and find its location and orientation (6 DOF). In the current paper color based tracking [15] is used. After the colour target is located then a numerical iterative method and TRIAD [16] based algorithms are used to precisely compute 6DOF. This information is given to kinematics to compute each joint angle with the help of inverse kinematics. In the second phase robotic manipulator is controlled based on inverse kinematics information available to move toward the planned grasping location, such that the robotic arm is ready to capture the target. The third phase consists in the actual capture (physical interception) phase in which the manipulator physically grasps the capturing device of the target satellite. The fourth phase is the post-capture phase, where the captured target is stabilized along with the servicing system. This paper [10] provides a survey of the literature on different topics related to space robotic systems for manned and unmanned on-orbit servicing missions.

3 BASIC BLOCK DIAGRAM OF THE SYSTEM

The system consists of a USB camera mounted on a robotic arm, control system electronics and a robotic arm with gripper and the corresponding drive electronics. The camera will see objects and will find out the colour marker location in the image frame. This data will be used to compute 6DOF information (3 translation and 3 rotation angle) . This data will be used with inverse kinematics to compute the joint angle of the robotic arm. The robotic arm will have rotation provision and the arm will be stopped based on distances which will be available from translation. Other two axis translation will be used to align the entire spacecraft so that robotic manipulator can grip and pull the other spacecraft. The control electronics will decide the required movement to reach the target depending on joint angle. The image processing pipeline is explained in Figure 2 .This process will be repeated till the robotic arm reached to the destination and able to grip the servicing satellite. The details step of the above block diagram is explained below.

3.1 Image processing pipeline

For a robotic arm to reach its needs very accurate and precise tracking. It should be fast, reliable and robust. For this purpose the colour marker tracking is used. Colour detection can be done much fast and reliable way compared to other feature tracking method. The input colour image has 3 component ,i.e. Red,Green,Blue. Initially it is converted to HSV(Hue, Saturation, Value) colour space Figure 3 . Here Hue is mainly used for colour thresholding. In the real image, other than the actual circular marker, it is possible some other small blobs of that particular hue may get detected. Those small blobs needs to be discarded for computation. Hence image clustering is used and they are arranged in ascending order of their size. The largest and 2^{nd} largest cluster (for red marker) and largest cluster for the blue marker will be selected for further computation. To identify the location of the marker centroid of the cluster is computed. So three centroid $(x_1, y_1), (x_2, y_2), (x_3, y_3)$ is available after image processing algorithm. This centroid location is used for 6DOF calculation using numerical techniques as explained subsequently (Figure 4).

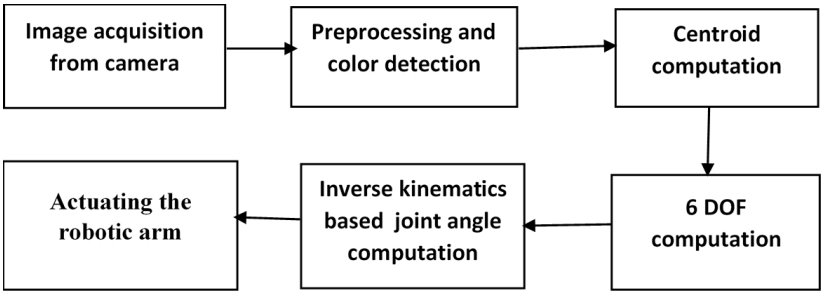

Figure 2: Robotic arm actuating pipeline

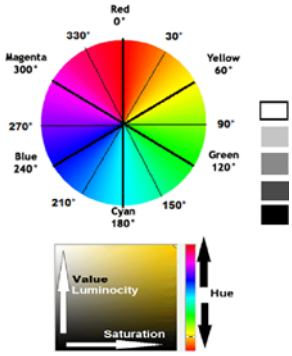

Figure 3: HSV Color space Source https://linzichun.com/posts/

3.2 6 DOF computation using TRIAD

To compute 6DOF , three color markers are mounted on a structure where two are in plane(Img2,Img3) and one are out of plane (Img1)(Figure 4). This out of plane marker will enhance the rotation accuracy. As explained earlier,($(x_1, y_1)$is the centroid location of the out of plane marker in the image and (x_2, y_2)&(x_3, y_3) are the centroid for Img2 and Img3 marker in the captured image. So initially for each such centroid, azimuth and elevations are computed and they are (α_1, β_1), (α_2, b_2), (α_3, β_3)respectively. This azimuth and elevation will be used to generate unit vector $(\boldsymbol{u}_1, \boldsymbol{u}_2, \boldsymbol{u}_3)$ for those three points. Then by finding dot product between two vectors, angles are calculated as follows

$$L_{12} = (\boldsymbol{u}_1.\boldsymbol{u}_2 \tag{1}$$

$$L_{23} = (\boldsymbol{u}_2.\boldsymbol{u}_3 \tag{2}$$

$$L_{13} = (\boldsymbol{u}_1.\boldsymbol{u}_3 \tag{3}$$

From the initial position of the marker location, the vector position is known in the target frame. k_{12}, k_{23},$k_{13}$are the distance between marker 1&2, 2&3,1&3 respectively. Now a vector R_{1x3}can be defined where R(1),R(2) & R(3) are the distances of color marker point from camera optical centre. Initially they are assumed same number with initial value. Now for each point three equations are formed and written in matrix form as below.

$$g = \begin{bmatrix} R(1)^2 + R(2)^2 - 2R(1)R(2)L_{12} - k_{12}^2 \\ R(2)^2 + R(3)^2 - 2R(2)R(3)L_{23} - k_{23}^2 \\ R(1)^2 + R(3)^2 - 2R(1)R(3)L_{13} - k_{13}^2 \end{bmatrix} \tag{4}$$

Now newton Raphson method is used for non linear optimization. The updated value of R_u will provide range information. Then azimuth and elevation will be used to compute X,Y,Z of each point. Now for each three point vectors are calculated in chaser $Img1_t$, $Img2_t$, $Img3_t$ is the position vector of $Img1$, $Img2$, $Img3$ color marker respectively. The vectors in the chaser frame will be

$$R12_c = R(1)\boldsymbol{u}_1 - R(2)\boldsymbol{u}_2 \;\&\; R13_c = R(1)\boldsymbol{u}_1 - R(3)\boldsymbol{u}_3 \tag{5}$$

The vectors in the target frame will be

$$R12_t = Img1_t - Img2_t \;\&\; R13_t = Img1_t - Img3_t \tag{6}$$

The chaser frame vectors are normalized and will be denoted as $(\boldsymbol{u12_c}, \boldsymbol{u23_c})$ and target frame vectors are normalized and denoted by $(\boldsymbol{v12_t}, \boldsymbol{v23_t})$, Now using the above vectors three triads are computed for chaser frame $(\boldsymbol{t1_b}, \boldsymbol{t2_b}, \boldsymbol{t3_b})$ and target frame $(\boldsymbol{t1_i}, \boldsymbol{t2_i}, \boldsymbol{t3_i})$**.** From these TRIAD rotation matrix can be computed and angles are extracted considering Euler 1-2-3 rotation.

3.3 Lab Calibration and stability:

The camera needs accurate lab calibration set up(Figure 5) to obtain a very high accuracy output. The camera is mounted on a rotation table to ensure zero rotation, zero translation. Then the image is captured (Figure 6) and camera optical centre is determined. Similarly, computation of focal length is also done based on FOV. Here the extrema two position images was captured by rotating the turn table and thus FOV is calculated. Using that focal length is computed. This information is used to determine 6 DOF information. A linear translator is used to verify the correctness of the translation movement. The 3σ stability plot was obtained for a particular position .Figure 7 shown stability along x, Figure 8 shows stability along y, Figure 9 stability along z.Camera was put stationary and all 3 axis translation are plotted with X axis as No of Sample and Y axis as translation. It is observed only along X axis (along the sensor optical axis) accuracy ~2mm and other two axis it is <0.5mm which indicates the detection method is robust and can provide accurate translation information.

4 SYSTEM DESCRIPTION

Chaser and Target satellites are two small satellites of size 0.5m x0.5m x 0.5m and mass of about 100kg each [8].The manipulator arm with 6 DOF(Figure 1) is mounted with the base of the shoulder joint being fixed to the Chaser Spacecraft.

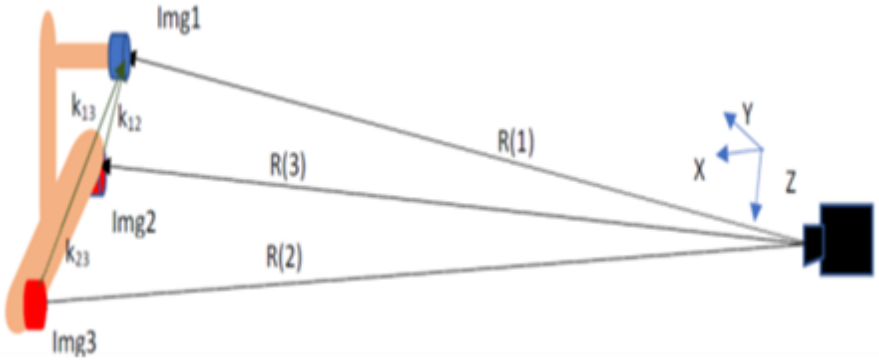

Figure 4: 6DOF calculation using camera

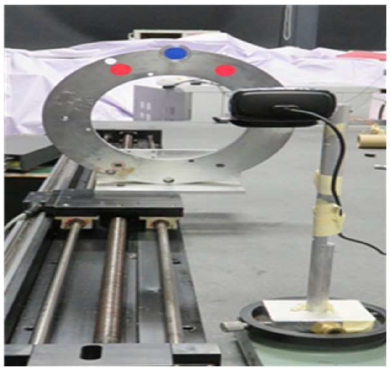

Figure 5: Lab set up for stability measurement

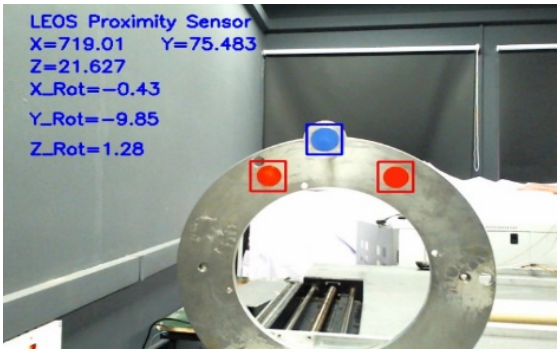

Figure 6: Images captured in Lab with color marker detected

The arm is consists of two links, Arm 1 & Arm 2 (Figure 10). The shoulder joint has two revolute joints, Joint 1 & Joint 2 which provides rotation about roll & pitch axis. The two links are connected by the elbow joint, Joint 3. At the end of Arm 2 is the wrist mechanism which provides for rotation about three perpendicular axes (Joints 4, 5 & 6) and constitutes a two finger gripper at its end which is meant for capturing the Target Spacecraft. The gripper consists of a ball screw and four bar mechanism for operating the two fingers which captures the grappling rod on the target Spacecraft.

5 ANALYSIS AND MODELLING

A berthing analysis has been carried out using ADAMS 2012 software for the evaluation of the motor torque requirements for the robotic arm. Berthing constitutes of two basic steps:

Capture: The maneuvering of the robotic arm to capture the target spacecraft.

Retraction: The maneuvering of the robotic arm to bring the grappled target within close proximity of docking mechanism.

The second step is more critical for the evaluation of the motor torque requirements as the inertia attached to the robotic arm is higher. The robotic arm is modeled in ADAMS with 6 rotational DOF as shown . All the six joints in the robotic arm are modeled with revolute joints. The motors of the robotic arm are considered to operate with a constant angular velocity of 1deg/sec. The robotic joint is mounted over the chaser spacecraft. The target spacecraft is modeled as a freely suspended body in space. During capture and retraction the moments at the joints are evaluated. The maximum initial relative velocity and angular velocity imparted to the target are 1mm/sec and 0.01deg/sec at the start of the movement of the robotic arm from the chaser. It is assumed that during the capture the thrusters are inactive thus rendering the chaser unstable while during retraction chaser spacecraft is stabilized by the thrusters. Hence during retraction analysis all the 6 DOF of the chaser are constrained [9]. The analysis is also carried out for the case where the thrusters are inactive during retraction. Inactivated thrusters can be simulated by releasing all the 6 DoF of the chaser spacecraft.All the three cases the maximum torque required by different motors are tabulated in the Table 1.

5.1 Case 1

For the first case the target spacecraft translates relative to the chaser spacecraft about the three translational axes with a magnitude of 1mm/sec each. The chaser spacecraft is constrained about all 6 DOF during retraction.

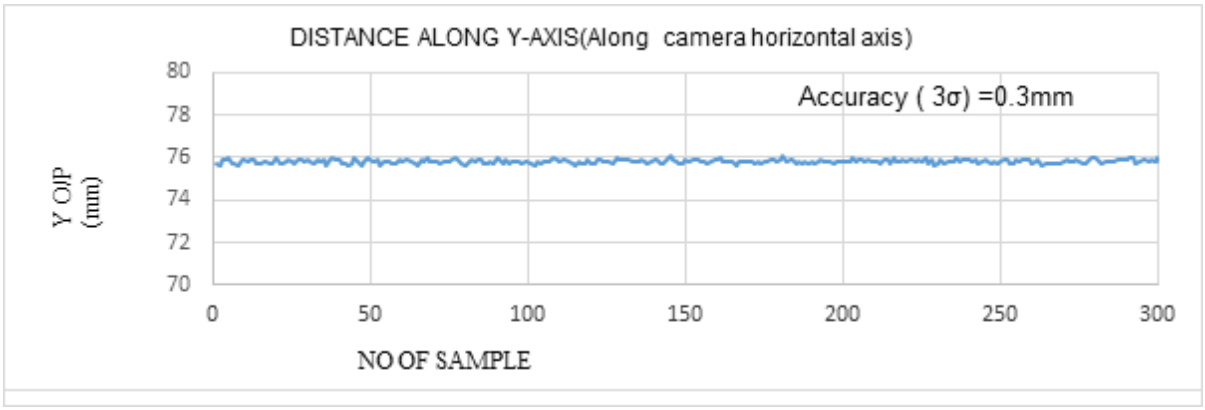

Figure 7: Stability plot along Y axis

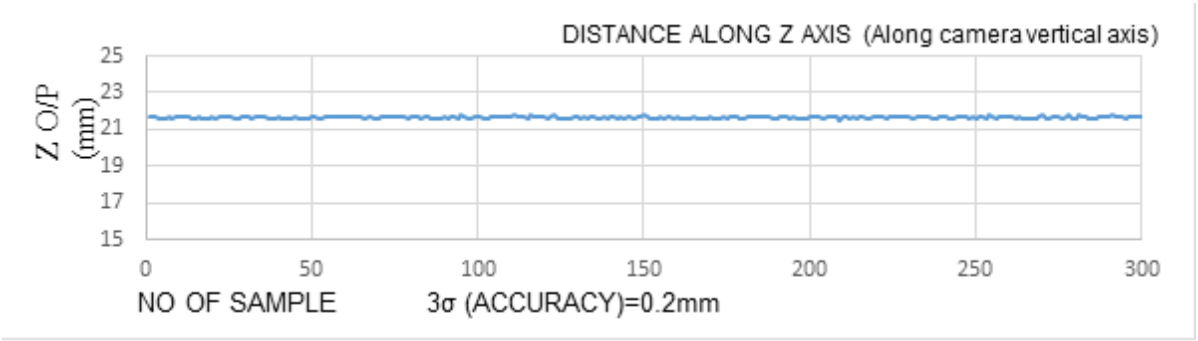

Figure 8: Stability plot along Z axis

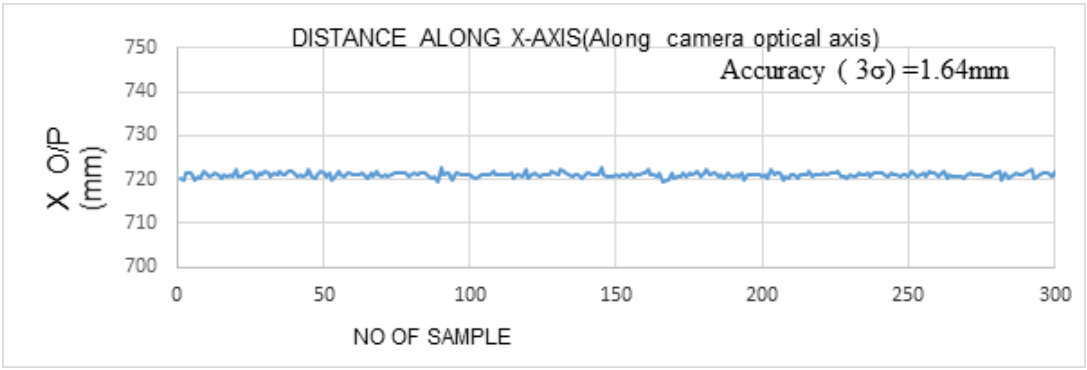

Figure 9: Stability plot along X axis

5.2 Case 2

For the second case in addition to imparting the relative translational velocities as in case-1 relative angular velocity of 0.01 deg/sec is also imparted to the target about the three axes with respect to the chaser. The chaser spacecraft is constraint about all 6 DOF during retraction.

5.3 Case 3

In first and second case the chaser spacecraft is stabilized by thrusters while in the third case the thrusters are inactive. Hence, chaser is in a free-free condition. The initial conditions are same as that of Case-2. The torque requirement for the motor gets reduced considerably.

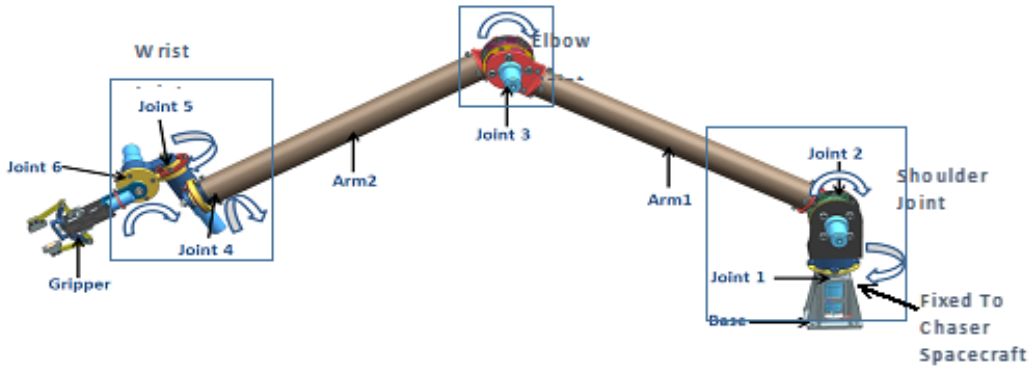

Figure 10: Configuration of the robotic arm

Table 1: Study of torque requirement for various configurations

Joint ID	Torque Requirement(Nm) Case1	Torque Requirement(Nm) Case2	Torque Requirement(Nm) Case3
1	1.2	2.5	0.4
2	2	5.0	0.45
3	2.6	3.5	0.85
4	1.9	1.9	0.85
5	1.8	1.35	0.39
6	0.4	0.2	0.3

5.4 Observations

Cases (1&2) where the chaser is constrained the reaction moments generated by the thrusters get transferred to the joints thus inducing greater load on the motors. While in case-3 all DOF of the chaser are released. Hence the chaser is in a free-free condition and the motor joints thereby see reduced torque requirements. During the analysis it is assumed that the motors operate at 1deg/sec. On reducing the operating speed, the torque requirement may further drop down. The torque requirements are maximum for Case-2 which were considered as design input for motor selection.To maintain motor at nominal operating temperatures foil heaters are bonded on the motor housing. The metallic components are anodized to keep temperatures within nominal ranges.

6 ROBOTICS DESIGN OF ARM

Design trade off and options study was performed to arrive at the final configuration of the manipulator arm [18].The manipulator arm consists of three important subassemblies: a) Shoulder and elbow joints b) Wrist mechanism c) End effector/Gripper Mechanism

6.1 Shoulder and elbow joints.

The configuration of both shoulder and elbow joints are kept similar based on their capability to drive higher inertia as compared to the wrist joints. Each joint is driven using a 6 Nm capacity BLDC motor with planetary gear head and encoders for position feedback. The motor shaft is supported on a pair of radial ball bearings to resist the moment loads coming due to the tip mass in fully stretched configuration at a distance of 1 m from the manipulator base. The bearings are kept in a preloaded condition by suitably tolerancing the mating components such as clamp, rotor bracket and spacer. The inner race of the bearing is mounted on the stator and the outer race is connected to the rotor. The rotor is coupled to the shaft using a single D joint to prevent any relative motion between the two parts.

6.2 Wrist Mechanism.

Minimum 6 Degrees of freedom (DOF) are required to capture target spacecraft in space by a free flying manipulator. Therefore Wrist mechanism consists of three non-intersecting joints to facilitate fine adjustment in all the three rotational axes required during operation. Since the moment load due to inertia is less at the wrist; smaller 1.5 Nm BLDC motor with planetary gear head and encoders is used to drive the joints. In wrist joint motor, shaft is coupled to an output shaft using a flexible metallic coupling to cater for any mismatch due to fabrication errors. Further the output shaft is supported on a pair of radial ball bearings similar to shoulder joints. Only difference is that the inner race of the bearing is connected to the rotating shaft and the outer race is connected to the stationary housing. At the end of the output shaft is a double D interface to connect the housing of the other wrist joint. Gripper mechanism is connected at the end of the third wrist joint.

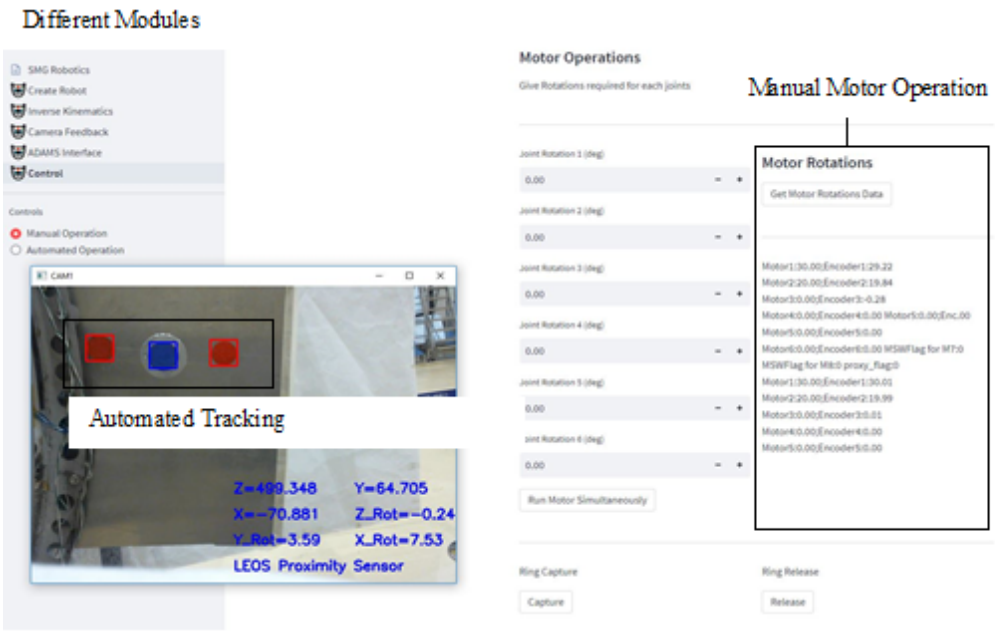

Figure 11: GUI of the software

6.3 Gripper Mechanism.

The gripper is actuated using a ball screw mechanism driven by a brush DC motor. As the motor rotates the screw & the nut pair can move linearly in either direction thus actuating the four bar mechanism which thereby either closes or opens the two fingers. The friction due to relative motion between the links is reduced by mounting a du bush at the joints. To provide a positive lock to the gripper a rest pad is provided which act as a third gripping point ensuring that the target is sufficiently inside the triangle formed by the rest pad and the two fingers. Gripper pads are connected at the tip of each finger which serves as a housing for sensors for gripper force measurement and acts as a non-contact type target locator.

7 TARGET RECOGNITION AND CAPTURING SOFTWARE

Target Recognition and Automated Capturing Software (TRACS) is developed to operate the robotic arm. Figure 11 shows the GUI of the developed software. The designed software has 5 modules.

1. The first module uses ETS to define a robotic arm. Any generalized robotic arm can be defined using this module with user defined degree of freedom. Once the robotic arm has been defined the software can be used to view the simplified model of the robotic arm as shown in Figure 12 .
2. The second module of the software does inverse kinematics for the defined robotic arm. It evaluates the motor rotations required for the robotic arm to transverse from the initial configuration to the required pose.
3. The third module of the software interfaces with the camera to receive the target position in real time.
4. The fourth module is interfaced with the drive electronics of the motor to arbitrarily command motor rotations.
5. The fifth module of the software integrates the first four modules to track the target automatically in real time and then capture the interface ring.
6. The software interfaces with the camera based pose estimation program to receive the pose of the camera mounted on the robotic arm w.r.t target. The evaluated transformation matrix can be inverted to get the pose of the target w.r.t camera. The encoders present in the motors provide individual rotated angles of each motors present in the robotic arm. Using the encoder data the pose of the robotic arm can be evaluated. The software calculates the following transformation matrix in real time during the tracking of the target.

${}^{capturing\ Pos}_{target}T$ = 4x4 transformation matrix of the capturing position on the ring w.r.t target (Defined by geometry)
${}^{target}_{camera}T$ = 4x4 transformation matrix of the target w.r.t camera (Evaluated using the camera feedback)
${}^{camerat}_{end\ effector}T$ = 4x4 transformation matrix of the camerat w.r.t End-effector (defined by geometry)
${}^{end\ effector}_{base}T$ = 4x4 transformation matrix of the End-effector w.r.t base (evaluated using the encoder feedback)

$${}^{capturing\ pos}_{base}T = {}^{capturing\ Pos}_{target}Tx^{target}_{camera}Tx^{camerat}_{end\ effector}Tx^{end\ effector}_{base}T$$

Product of the transformation matrix of the robotic arm and the target w.r.t the camera gives the overall transformation matrix of the target w.r.t base of the arm. The software takes feedback from the encoder data and from the camera and in real-time derives the current pose of the robotic arm as well as the transformation

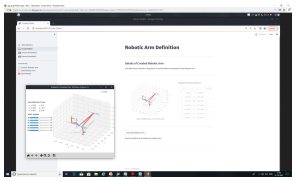

Figure 12: Simplified view of robotic arm by software

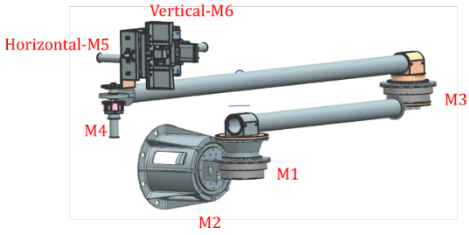

Figure 13: Robotic arm manipulator with all joints

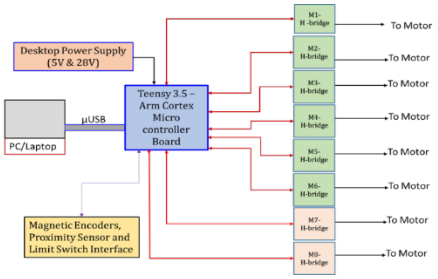

Figure 14: Drive hardware block diagram

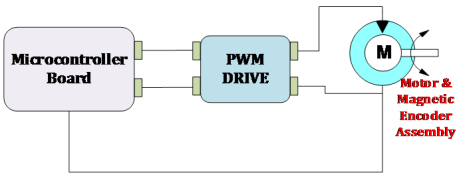

Figure 15: Control loop diagram

matrix for the gripper to reach the target.The software uses inverse kinematics to evaluate the additional rotations required by the motors reach the target. The software commands the motor to operate for the required angles. These steps are executed in a loop as long as the distance between the target and the gripper is within the set tolerance limit or the proximity sensor in the gripper gets actuated. Once the tracking of target is over, time based series of commands are run to operate the gripper for capturing the target. On successful capture of the target the robotic arm is brought to its rest pose along with the target.

8 ROBOTIC ARM AVIONICS

Drive Electronics is built to cater for driving 8 Brushed DC Motors (BDC) simultaneously in close loop. Major components of avionics include Teensy 3.5 board (32bit-120MHz Arm cortex-M4 floating point microcontroller), Dual-H-bridges (L298) and other peripheral circuitries. Out of eight motors, six are for arm joints, two are for gripper. Six arm motors include two at shoulder (246:1 gear train), one at elbow (158:1 gear train), and three at wrist (158:1 gear train). Figure 13 shows robotic arm configuration with all motors nomenclature. Each ARM-BDC motor is housed with incremental magnetic encoder to provide real time shaft position. These are 9 bit encoders. Encoder signals (A & B) are captured and processed by microcontroller. By processing both rising and falling edge of encoder signals, the positional resolution is further enhanced by 4 times. For a full motor range of 360°, encoder provides resolution as 0.176°.

$$Encoder\ Resolution = \frac{360^\circ}{4 * \left(2^9 - 1\right)} \cong 0.176^\circ$$

8.1 Drive Electronics Design & Realization

Figure 14 shows basic block diagram and interfaces of drive electronics.All motors are powered with single 42V power supply. Pulse-width-modulation (PWM) based variable speed controller is implemented to run each motor at different voltage and speed. All six arm motors are controlled using PD controller (position and rate control) with encoder in close loop based on commanded angle. Figure 15 shows control loop block diagram.Innovative mixed braking mechanism (mixture of slow and fast braking) for BDC motor is implemented in this design which avoids free running of motor when supply is cut-off. Each motor module has limit switches at either end. These limit switches get activated once motor shaft comes in contact with them. When these limit switches are activated, respective motor rotation is stopped. Proximity sensor interface is also included in this hardware. Proximity sensor is triggered when robotic arm reaches near the target, thereby switching off all the six arm motors.Gripper motors comprise of one horizontal actuator and one vertical actuator. These gripper motors are controlled based on commanded run-time & individual limit switches.

8.2 Implementation:

Drive Software is implemented using Embedded C/C++ language using Arduino IDE. Software has provision of commanding absolute angles (±360° range), with added features such as presetting of present angle, pulse width selection (Resolution: 1us, up to seconds), enabling or disabling limit switches and proximity sensors logics etc. Modes of operation include idle, start, abort, pause, and resume options. GUI has been developed for commanding and telemetry acquisition of encoder positions, limit switch positions etc.

9 TESTING

Testing to be done with over all zero g fixture .In this method, the centre of gravity of the 2 arms and the wrist are found out individually using the CAD. In this case, the weight of the robotic manipulator may be offloaded by attaching counter balance at required points using pulleys connected on guide rails of overhead zero-g setup or bungee cord system. All 6 DOF of the robotic arm may be demonstrated using this set up (Figure 16).

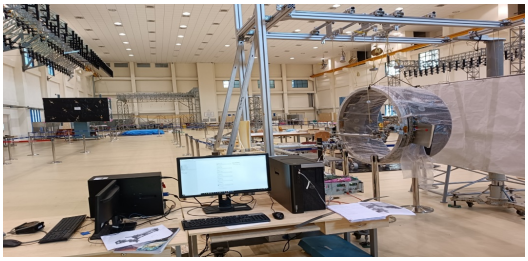

Figure 16: Overhead Zero g set up

10 CONCLUSION

In this paper, a method to compute 6 DOF freedom using color target is presented and test results are shown. The output was interfaced with inverse kinematics software to generate joint angle for robotic arm. Various aspects and design of robotic manipulator design, joint types were simulated and fabricated and tested in an integrated way. The method and test results are explained in this paper. This method can be used for On Orbit service of the spacecraft with suitable modification.

11 FUTURE WORK

For future version, it is proposed improve the vision based detection algorithm with some existing feature and detect similar or better accuracy. Avionics can be improved with Brushless DC (BLDC) motor based 6 DoF robotic arm. State space based BLDC motor control with Hall sensor/magnetic encoder in closed loop will be the implemented for the same. The prime challenge will be sizing of BLDC motor with gear train.

REFERENCES

[1] Abhinandan Kapoor and R. Ranganath, “Space Robotics – A Brief Overview”, Association for Machines & Mechanisms Bulletin, Volume 6, No. 2, April 2014

[2] AarataEjiri, Ichiro Watanabe, KeijuOkabayashiet.al.,“Satellite berthing experiment with two armed spacerocket”, Space systems laboratory, Fujitsu Laboratories Ltd, Kawasaki, 211 Japan

[3] Lakshminarayana, B., Ranganath, R., and Nataraju, B. S.,“Studies on Docking Dynamics using ADAMS”, Journal of Spacecraft Technology, Vol. 10, No. 1, Jan 2000, pp. 40 to 51.

[4] WenfuXu, Bin Liang, WenyiQiang, et.al. ,"Trajectory Planning of space robot system for target berthing and reorientation after capturing", Proceedings of the 6th World Congress on Intelligent Control and Automation, June 21- 23,2006, Dalian, China

[5] Seweryn Karol, Banaszkiewicz Marek, MaedigerBernd ,et.al. ," Dynamics of space robotic arm during interactions with non-cooperative objects", ESA/ESTEC, NOORWWIJK, THE NETHERLANDS / 12-14 APRIL 2011

[6] P. Rank, Q. Muhlbauer, W. Naumann, K. Landzettel ," The DEOS Automation and robotics payload", ESA/ESTEC, NOORWWIJK, THE NETHERLANDS / 12-14 APRIL 2011

[7] Oda Mitsushige, Kawano Isao, KibeKouichi, Yamagata Fumio, ETS-7, "A Rendezvous Docking and Space Robot Technology Experiment Satellite-Result of the Engineering model development work", IEEE

[8] R. Ranganath and C. D. Sridhara," Development of a Mechanism for Autonomous Docking of Spacecraft", The National Conference on Space Transportation Systems: Oppurtunities and Challenges (STS 2011),Tiruvananthapuram from Dec 16 to 18, 2011.

[9] SidharthTiwary,B. Lakshminarayana, R. Ranganath, G. Nagesh and C.D. Sridhara, “Studies on the Dynamics of Spacecraft Berthing”, ARMS, Pune, 2012.

[10] Flores-abad A., Ma O., Pham K., Ulrich S. (2014). A Review of Space Robotics Technologies for On-Orbit Servicing. *Prog. aerospace Sci.* 68, 1–26. 10.1016/j.paerosci.2014.03.002

[11] Aghili F. (2012b).Active Orbital Debris Removal Using Space Robotics. In Proc. of International Symposium on Artificial Intelligence, Robotics and Automation in Space i-SAIRAS. Italy: Turin.

[12] Aghili F. (2012). A Prediction and Motion-Planning Scheme for Visually Guided Robotic Capturing of Free-Floating Tumbling Objects with Uncertain Dynamics. *IEEE Trans. Robotics* 28 (3), 634–649. 10.1109/tro.2011.2179581

[13] Aghili F. (2020). Energetically Consistent Model of Slipping and Sticking Frictional Impacts in Multibody Systems. *Multibody Syst. Dyn.* 48, 193–209. 10.1007/s11044-019-09703-2

[14] Flores-Abad A., Zhang L., Wei Z., Ma O. (2017). Optimal Capture of a Tumbling Object in Orbit Using a Space Manipulator. *J. Intell. Robot Syst.* 86 (2), 199–211. 10.1007/s10846-016-0417-1

[15] Suzuki, S., Tanaka, H., Narita, S., Watanabe, K., Ueta, A., Wada, M., Matsumura, Y. and Morimoto, H., 2016, June. The first experiment of a high-accuracy 2D color marker in space. In *Proceedings of the international Symposium on Artificial Intelligence, Robotics and Automation in Space (i-SAIRAS 2016).*

[16] Camille Pirat, Finn Ankersen, Roger Walker, Volker Gass, Vision Based Navigation for Autonomous Cooperative Docking of CubeSats,Acta Astronautica,Volume 146,2018,Pages 418-434,ISSN 0094-5765,1.

[17] Kawamoto S., Nishida S., Kibe S. (2003). *Research on a Space Debris Removal System.* Japan: NAL Res ProgNational Aerospace Lab.

[18] Abhinandan Kapoor et.al., Analysis & Design of a 6-DOF Robotic manipulator for Assisted Docking Experiment, ARMS 2015